



# Comparative Analysis of Edge Detection Techniques for Medical Images of Different Body Parts

Bhawna Dhruv<sup>1</sup>(✉), Neetu Mittal<sup>1</sup>, and Megha Modi<sup>2</sup>

<sup>1</sup> Amity University, Noida, UP, India

Bdhruv08@gmail.com, Savini09@gmail.com

<sup>2</sup> Yashoda Super Specialty Hospital, Ghaziabad, UP, India

Dr.meghamodi@gmail.com

**Abstract.** Medical images are arduous to process since they possess distinct modalities. Therefore, the medical practitioners cannot competently detect and diagnosis the diseases in conventional ways. There should be a system which helps physicians to understand medical images very easily. Image segmentation using edge detection is commonly used for image analysis and better visualization of medical images. Various methods have been used for image segmentation such as Threshold detection, Region detection, Edge detection and Clustering technique. Edge detection is one of the prominently used methods for segmentation. This technique focuses on identifying and analyzing the entire image based upon the detected edges. In this paper, MRI images of human body parts such as abdomen, ankle, elbow, hand, knee, leg, liver and brain are considered for edge detection. Further, filtering has been performed on the segmented images to remove the unwanted noise. This makes the image more clearly for further reference. The effectiveness of the proposed technique has been evaluated quantitatively by using the performance measures like Entropy and Standard Deviation. The proposed technique may be highly beneficial for medical practitioners to carry out the diagnosis for effective treatment.

**Keywords:** Image segmentation · Medical images · MRI · Edge detection  
Entropy · Standard deviation · Noise removal

## 1 Introduction

With the modern approach in the field of information technology, the revision in the analysis of the medical images has devoted noticeably to the early diagnosis of various diseases. Image segmentation especially edge detection technique give much knowledge that help to explain the medical images and improve the sharpness of detection and further diagnosis of different diseases. Image Segmentation is the process of dividing an image into meaningful structures where each pixel has same attributes [1]. The pixel is similar on the basis of criteria such as texture, color or intensity. Image segmentation aims at improving the pictorial information for interpretation. This process can be achieved by converting a low level image into high level image which may deem to be a challenging task as an image is never partitioned accurately for analysis [2]. One of the

processes of achieving the same is through Edge detection techniques. The reason behind implementing an edge detector to a set of images is highly suggestive of reduction in amount of data to be processed. This further overlooks insignificant data and captures important properties of an image. Various types of edge detection operators such as Sobel, Roberts, Prewitt, Canny and LoG can be applied to study the results on a particular image [3]. The aim of the paper is to study these edge detection techniques and apply them on the MRI images of different body parts to analyze the results. Image Segmentation plays a vital role in medical image processing, particularly for different body parts abnormalities detection in Magnetic Resonance Imaging (MRI) and computed Tomography (CT). The idea behind using MRIs to CT is that the latter doesn't use ionizing radiations, hence giving us a clear picture of the health condition [4]. The results are based upon three parameters i.e. Entropy, Standard Deviation and Execution Time. Entropy, generally defines the amount of information which must be used to compress the image by any compression algorithm [5]. Similarly, the standard deviation explains the variation of the results from the actual value of any parameter in an image.

Moreover, image seized from different sources suffer deterioration which affect the essential features of the image and makes image study difficult. Image restoration attempts to restore the degraded images by removing noise from the image. The process of image restoration completely depends upon accuracy of image analysis and generally removes unwanted pairs [6]. It studies entire degradation process and evaluates the inverse process to assess the original image. It is an objective process and restores the approximation of actual image.

In this paper Edge detection techniques are applied with different operators on MRI images.

#### A. Magnetic Resonance Imaging:

Magnetic Resonance Imaging (MRI) is a medical imaging technique used to visualize detailed internal structures of respective body part with the help of magnetic radiation. It provides three dimensional real-time views of organs mostly for the soft-tissue. It furnishes good contrast of soft tissue, gives better visualization of soft-tissue structures like brain, spine, muscles, and joints. The MRI machine used to capture in multiple body planes without changing the physical positions of the patient under scanning as it operates in multiple planes. Image segmentation may be widely used in MRI images of brain to detect tumor and other skin lesion or patches like abnormalities. Also Image segmentation on MRI images is also useful after surgery to keep sign the improvement of treatment and to monitor the growth of tumor before surgery.

## 2 Edge Detection Technique

Edge detection has turned out to be most competent field in image processing which helps in locating sharp discontinuities in an image. These discontinuities are blunt changes in the intensity of pixels which define the edges of image [7]. The edge element is crucial and significant feature of an image. There are several edge detection techniques depending upon the sensitivity of an image which are designed to work

upon in vertical, horizontal and diagonal directions [8]. It must be noted that the preferred direction of every convolution mask is weighted with highest coefficients. Apart from edge detection, noise removal also plays an important role in image processing. The goal of removing noise is to discard unwanted pixels.

Different edge detection operators:

A. *SOBEL*:

The Sobel operator is used to perform spatial gradient measurement on any image. It is used for edge detection of two basic types i.e. Vertical Direction and Horizontal Direction [9]. This operator consists of  $3 \times 3$  convolution mask which is designed in such a way that every edge whether in vertical or horizontal direction is detected relative to the pixel grid [10]. The convolution mask of the image is generally smaller as compared to the actual image. These masks can be applied in any form i.e. Corresponding to  $G_x$  or  $G_y$  separately or together so as to give an absolute gradient measurement at each point. The intensity of the function at eight distinct points is recognized to sample image point. The  $G_x$  mask highlights the horizontal edges in the image while  $G_y$  highlights the vertical edges, it further calculate the difference between pixel intensities of the particular direction [11]. As it is visible from the mask, the zeros in the middle row helps to compute the difference between the intensities of the edge [12]. This operator is disrupted by noise easily, therefore cannot detect outermost images easily. The basic advantage of using this operator is that weights can be applied to the coefficients which produce better result.

$$\begin{aligned}
 |G| &= \sqrt{G_x^2 + G_y^2} \\
 G_x &= \sum \sum Sobel_{x,i,j} * I_{r+i-2,c+j-2} \\
 G_y &= \sum \sum Sobel_{y,i,j} * I_{r+i-2,c+j-2}
 \end{aligned}$$

B. *ROBERTS*:

The Roberts operator is used to highlight the high spatial frequency of the corresponding edges of any image. The kernels used for this operator are rotated by  $90^\circ$  therefore the convolution mask is designed to give the maximum results of the edges running at  $45^\circ$ . Similar to Sobel Operator, the edges can be detected separately or absolute gradient can be computed by combining  $G_x$  and  $G_y$  [13]. The convolution masks are given below:

$$|G| = \sqrt{G_x^2 + G_y^2}$$

Robert also proposed the following equation:

$$\begin{aligned}
 y_{i,j} &= \sqrt{x_{i,j}} \\
 z_{i,j} &= \sqrt{(y_{i,j} - y_{i+1,j+1})^2 + (y_{i+1,j} - y_{i,j+1})^2}
 \end{aligned}$$

- x: Initial density of the image.  
 z: Computed derivate.  
 i, j: Location of image.

### C. PREWITT:

This technique was devised to conquer the problems of Sobel operator i.e. absence of smoothing modules. It detects the edges in both vertical and horizontal direction which is a way of finding the approximations in magnitude and orientation of the edge in an image [14]. It has maximum 8 possibilities of orientation and does not emphasize on central value of the mask. The kernels of this operator are of least values thereby preventing blurring and extra trouble. The convolution mask is given below:

$$|G| = \sqrt{G_x^2 + G_y^2}$$

$$\text{Also, } G = \sqrt{G_x^2 + G_y^2} \theta = \text{atan2}(G_y, G_x)$$

### D. CANNY:

This edge detection technique is also known as optimal edge detector as it focuses on improving the results as compared to the other operators [15]. This initially smoothes the image and removes the noise and then gives the output of spatial gradient measurement on any image. This filter helps to smoothen the noise as well detects the edges meticulously. It works to satisfy the conditions like localization of edge, low error rate and single edge detection. The gradient is calculated using the Gaussian filter [16]. The edge identification image is then exhibited to thresholds followed by the process of hysteresis to suppress the non suppressed pixels.

### E. LoG:

The laplacian of Gaussian is 2D isotropic measure of 2nd special derivative of the image which focuses on highlighting the region where the intensity of the image changes very rapidly [17]. Therefore this is a highly used edge detection technique. The operation of this detector works in a way that it first smoothes the noise using the Gaussian filter and then gives the output as a gray image only [18]. The laplacian of an image is as given below:

$$L(x, y) = \frac{\partial^2 I}{\partial x^2} + \frac{\partial^2 I}{\partial y^2}$$

As it can be seen that all the three filters deal with second derivate measurement of the image, it becomes necessary to first smoothen the image so as to reduce the noise and then the Gaussian filter is applied [19, 20].

### 3 Measuring Parameters of Image Analysis

The quality of any image can be determined on two basis i.e. subjective or objective. The subjective as the name suggests consumes more time as compared to the latter. In our work, we have considered two quantity measures as given:

#### A. Standard Deviation:

The standard deviation is the measure of distribution of the set of data from its mean. It measures the absolute instability of a distribution [21, 22]. Higher instability depicts higher standard deviation. Generally, continuous data is required to calculate standard deviation. It is given by:

$$\sigma = \sqrt{\sum_{i=0}^L (i - \bar{i})^2 h_f(i), \dots \bar{i} = \sum_{i=0}^L i h_f}$$

#### B. Entropy:

Entropy as defined by the Math works is a statistical measure of randomness that can be used to characterize the texture of input image [23]. Images with low entropy have low contrast whereas high entropy depicts high contrast in an image but are troublesome to compress. It is given by:

$$E = - \sum_{i=0}^{L-1} p_i \log_2 p_i$$

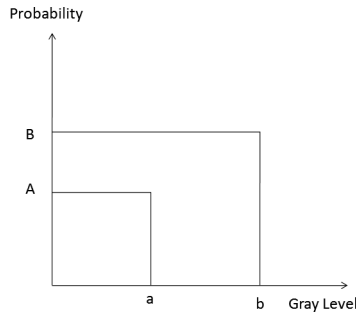
In our work, we have dealt with the MRI images of different body parts. MRI (Magnetic Resonance Imaging) is a medical imaging technique used in radiology to form pictures of the anatomy and the physiological processes of the body in both health and disease. On the images of different body parts, several operators have been applied to study the result.

### 4 Noise Removal

Digital images play fundamental role in the field of research, medical imaging and information systems using satellites. The images collected from distinct sources are noisy hence de-noising techniques are applied so as to achieve better results for analysis. De-noising still prevails as a challenge in the research therefore techniques like image enhancement are used to improve the image quality. The filtering techniques are treated as first step to obtain images rich in quality.

*A. Salt and Pepper:*

The pixels in the image get destroyed due to transformation from analog to digital domain. These corrupted images are known as impulse noise which are of two types i.e. fixed value impulse noise and Random value impulse noise. The fixed impulse noise is also referred to as Salt and Pepper which accepts only 2 values, either 0 for pepper or 255 for salt. The random value impulse noise whereas can accept any value ranging from 0 to 255. This noise generally occurs in an image due to defects in camera’s sensor cell or synchronization errors (Fig. 1).



**Fig. 1.** Probability density functions of salt and pepper noise

*B. Wiener:*

When an image is blurred using a low pass filter, the original image can be obtained by using the process of inverse filtering, however this process invites additive noise to the image. The wiener filter optimizes inverse filtering and noise smoothing. It not only discards the noise but also performs inverse filtering. Wiener filtering in Fourier domain can be expressed as:

$$W(f_1, f_2) = \frac{H * (f_1, f_2) S_{xx}(f_1, f_2)}{(|H(f_1, f_2)|)^2 S_{xx}(f_1, f_2) + S_m(f_1, f_2)}$$

While performing image restoration using wiener filter, a low pass filter as shown below is used to blur the image.

$$H = 1/16 \begin{bmatrix} 1 & 1 & 1 & 1 \\ 1 & 1 & 1 & 1 \\ 1 & 1 & 1 & 1 \end{bmatrix}$$

The implementation of this filter requires the calculation of power spectra of both original image as well as additive noise. Power spectrum can be calculated using:

$$S_{yy}^{per} = \frac{1}{N^2} [Y(k, l)Y(k, l)^*]$$

Where,  $Y(k, l)$  is DFT of observation.

The technique of wiener filter is not highly used but produces best mathematical results.

### C. Poisson Noise:

It is an ambiguous association with the measurement of light and independence of photon detection. This noise contributes in varying proportion in an image. This generally occurs when the number of photons is not able to provide exact statistical information. It is also known as photon noise and is signal dependent whose magnitude increases with respect to intensity of light.

## 5 Simulation and Results

MRI images of different body parts such as abdomen, ankle, elbow, hand, leg, liver and brain have been taken for analysis. Edge detection operators such as Roberts, Sobel, Prewitt, Canny and LoG have been applied to each image. Further Entropy, Standard Deviation and Execution time is evaluated from the resultant images. Table 1 depicts the results obtained from the same highlighting prominent changes in the values of parameters especially in case of Laplace of Gaussian operator.

From the results shown in Table 1, it is clearly indicated that there are noticeable changes in the values of Entropy, Standard Deviation and Time for LoG operator.

For abdomen, entropy of original image is 4.0522. Different filters have been applied for analysis such as Robert, Sobel, Prewitt, Canny, LoG. Entropy of resultant images after applying filters are different from original image such as 4.0522, 0.1539, 4.0522, 4.0522, 4.0522, and 4.0757 are the entropy of different operators respectively.

For ankle, entropy of original image is 7.0966. Entropy of resultant images after applying filters are different from original image such as, 0.1887, 7.0966, 7.0966, 7.0966, 7.0966 and 6.9408 are the entropy of different operators respectively.

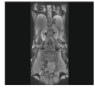




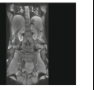





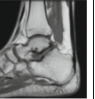
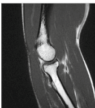




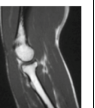






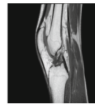



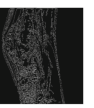

For elbow, entropy of original image is 6.2733. Entropy of resultant images after applying filters are different from original image such as, 0.1741, 6.2733, 6.2733, 6.2733 and 6.0439 are the entropy of different operators respectively.

For hand, entropy of original image is 4.9325. Entropy of resultant images after applying filters are different from original image such as 0.1642, 4.9325, 4.9325, 4.9325 and 4.5715 are the entropy of different operators respectively.

For knee, entropy of original image is 4.1647. Entropy of resultant images after applying filters are different from original image such as, 0.1490, 4.1647, 4.1647, 4.1647 and 4.5715 are the entropy of different operators respectively.

For leg, entropy of original image is 5.2013. Entropy of resultant images after applying filters are different from original image such as, 0.1446, 5.2013, 5.2013, 5.2013 and 5.3754 are the entropy of different operators respectively.

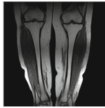




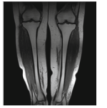
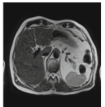
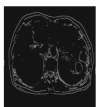
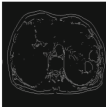
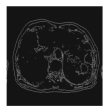

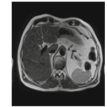
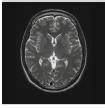




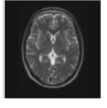
**Table 1.** Analysis of different operators on MRI of different body parts

Image	Original Image	Roberts	Sobel	Prewitt	Canny	LoG
Abdomen						
Entropy	4.0522	0.1539	4.0522	4.0522	4.0522	4.0757
Standard Deviation	44.0048	0.1475	44.0049	44.0049	44.0049	43.4800
Execution Time (In Sec)	0.116400	1.849964	0.950286	1.977930	2.329548	0.292388
Ankle						
Entropy	7.0966	0.1887	7.0966	7.0966	7.0966	6.9408
Standard Deviation	64.1354	0.1674	64.1356	64.1356	64.1356	62.0044
Execution Time (In Sec)	0.025406	0.364964	0.166824	0.294917	0.320282	0.056844
Elbow						
Entropy	6.2733	0.1741	6.2733	6.2733	6.2733	6.0439
Standard Deviation	52.2844	0.1593	52.2846	52.2846	52.2846	49.7832
Execution Time (In Sec)	0.027801	0.291431	0.195056	0.571107	0.373559	0.067847
Hand						
Entropy	4.9325	0.1642	4.9325	4.9325	4.9325	4.5715
Standard Deviation	56.3903	0.1536	56.3903	56.3903	56.3903	54.3642
Execution Time (In Sec)	0.053466	0.866227	0.426349	0.789168	0.898489	0.145112
Knee						

*(continued)*



**Table 1.** (continued)

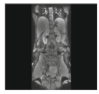




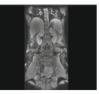






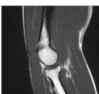




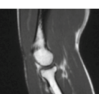












Image	Original Image	Roberts	Sobel	Prewitt	Canny	LoG
Entropy	4.1647	0.1490	4.1647	4.1647	4.1647	4.1790
Standard Deviation	68.6057	0.1446	68.6057	68.6057	68.6057	68.1572
Execution Time (In Sec)	0.148529	2.613820	1.324256	2.792228	2.453288	0.388934
Leg						
Entropy	5.2013	0.1446	5.2013	5.2013	5.2013	5.3754
Standard Deviation	48.0656	0.1419	48.0659	48.0659	48.0659	46.5672
Execution Time (In Sec)	0.055868	1.365116	0.520580	0.919118	1.057049	0.156223
Liver						
Entropy	5.8791	0.1870	5.8791	5.8791	5.8791	5.9122
Standard Deviation	52.0688	0.1665	52.0688	52.0688	52.0688	50.2168
Execution Time (In Sec)	0.055593	1.286821	0.472204	0.866820	1.024173	0.151872
Brain						
Entropy	5.0652	0.2291	5.0652	5.0652	5.0652	5.1647
Standard Deviation	39.4291	0.1891	39.4293	39.4293	39.4293	34.3848
Execution Time (In Sec)	0.019450	0.209662	0.137743	0.207306	0.186673	0.048438

For liver, entropy of original image is 5.8791. Entropy of resultant images after applying filters are different from original image such as, 0.1870, 5.8791, 5.8791, 5.8791 and 5.9122 are the entropy of different operators respectively.

For brain, entropy of original image is 5.0652. Entropy of resultant images after applying filters are different from original image such as, 0.2291, 5.0652, 5.0652, 5.0652 and 5.1647 are the entropy of different operators respectively.

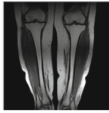




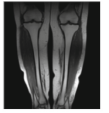
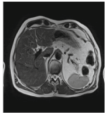
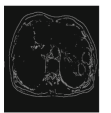
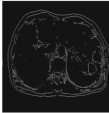
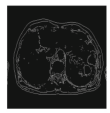

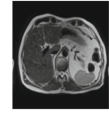
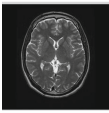




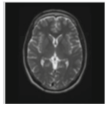
Further noise removal techniques have been applied to perform image restoration on the above resulting images to perceive and conclude the development of best operator and better image quality. Table 2 explains the noise removal techniques with

**Table 2.** Noise removal techniques with different operators on resultant images of Table 1

Image	Original Image	Robert	Sobel	Prewitt	Canny	LoG
Abdomen						
Entropy	4.0522	0.1539	4.0522	4.0522	4.0522	4.0757
Standard Deviation	44.0048	0.1475	44.0049	44.0049	44.0049	43.4800
Execution Time (In Sec)	0.116400	1.849964	0.950286	1.977930	2.329548	0.292388
Ankle						
Entropy	7.0966	0.1887	7.0966	7.0966	7.0966	6.9408
Standard Deviation	64.1354	0.1674	64.1356	64.1356	64.1356	62.0044
Execution Time (In Sec)	0.025406	0.364964	0.166824	0.294917	0.320282	0.056844
Elbow						
Entropy	6.2733	0.1741	6.2733	6.2733	6.2733	6.0439
Standard Deviation	52.2844	0.1593	52.2846	52.2846	52.2846	49.7832
Execution Time (In Sec)	0.027801	0.291431	0.195056	0.571107	0.373559	0.067847
Hand						
Entropy	4.9325	0.1642	4.9325	4.9325	4.9325	4.5715
Standard Deviation	56.3903	0.1536	56.3903	56.3903	56.3903	54.3642
Execution Time (In Sec)	0.053466	0.866227	0.426349	0.789168	0.898489	0.145112
Knee						

(continued)

**Table 2.** (continued)

<b>Entropy</b>	4.1647	0.1490	4.1647	4.1647	4.1647	4.1790
<b>Standard Deviation</b>	68.6057	0.1446	68.6057	68.6057	68.6057	68.1572
<b>Execution Time (In Sec)</b>	0.148529	2.613820	1.324256	2.792228	2.453288	0.388934
<b>Leg</b>						
<b>Entropy</b>	5.2013	0.1446	5.2013	5.2013	5.2013	5.3754
<b>Standard Deviation</b>	48.0656	0.1419	48.0659	48.0659	48.0659	46.5672
<b>Execution Time (In Sec)</b>	0.055868	1.365116	0.520580	0.919118	1.057049	0.156223
<b>Liver</b>						
<b>Entropy</b>	5.8791	0.1870	5.8791	5.8791	5.8791	5.9122
<b>Standard Deviation</b>	52.0688	0.1665	52.0688	52.0688	52.0688	50.2168
<b>Execution Time (In Sec)</b>	0.055593	1.286821	0.472204	0.866820	1.024173	0.151872
<b>Brain</b>						
<b>Entropy</b>	5.0652	0.2291	5.0652	5.0652	5.0652	5.1647
<b>Standard Deviation</b>	39.4291	0.1891	39.4293	39.4293	39.4293	34.3848
<b>Execution Time (In Sec)</b>	0.019450	0.209662	0.137743	0.207306	0.186673	0.048438

different operators such as Robert, Sobel, Prewitt, Canny, LoG applied on resultant image from Table 1.

From the results shown in Table 2, it is clearly indicated that there are noticeable changes in the values of Entropy, Standard Deviation and Time for LoG operator.

For abdomen, Entropy of the original image is 4.0522 and 4.0757 for LoG operator. For ankle, the entropy of original image is 7.0966 and 6.9408 for LoG operator. For elbow, the entropy of original image is 6.2733 and 6.0439 for LoG operator. For hand, the entropy of original image is 4.9325 and 4.571 for LoG operator. For knee, the entropy of original image is 4.1647 and 4.1790 for LoG operator. For leg, the entropy

of original image is 5.2013 and 5.3754 for LoG operator. For liver, the entropy of original image is 5.8791 and 5.9122 for LoG operator. For brain, the entropy of original image is 5.0652 and 5.1647 for LoG operator.

## 6 Conclusion

Although edge detection is an initial step in reviewing an image but it becomes crucial to understand different types of edge detection techniques. On the basis of the analysis of different MRI images, it is clear that LoG proves to provide better results as compared to Roberts, Sobel, Prewitt and Canny. The operators can be localized as per the requirement of a user to conform to an environment. Similarly the noise removal techniques also are essential to produce a relevant analysis and study of the images, in support of this, the results of the same give us a clear picture that wiener filter continues to give better results, although there are minute variations but they play very important role in detection algorithms and noise removal techniques.

## References

1. Singh, H., Agrawal, D.: A meta analysis on content based image retrieval system. In: Proceedings of the IEEE International Conference on Emerging Technological Trends, pp. 1–6 (2016)
2. Khader, A., Ali, A., Alfaki, A.: Color and texture fusion-base method for content-based image retrieval. In: Proceedings of the IEEE International Conference on Computing for Sustainable Global Development, pp. 3205–3210 (2016)
3. Patel, J.M., Gamit, N.C.: A review on feature extraction techniques in content based image retrieval. In: IEEE International Conference on Wireless Communications, Signal Processing and Networking, pp. 2259–2263 (2016)
4. Manno, A.: Content based image retrieval using salient orientation histograms. In: IEEE International Conference on Image Processing, pp. 2480–2484 (2016)
5. Zaitouna, N.M., Aqelb, M.J.: Survey on image segmentation techniques. *Procedia Comput. Sci.* **65**, 797–806 (2015). International Conference on Communication, Management and Information Technology
6. Kabai, L., Abdellaoui, M.: Content based image retrieval using local and global feature extractor. In: IEEE International Conference on Advanced Technologies for Signal and Image Processing, pp. 151–154 (2016)
7. Mageswari, S.U., Sridevi, M., Mala, C.: An experimental study and analysis of different image segmentation techniques. *Procedia Eng.* **64**, 36–45 (2013). International Conference on Design and Manufacturing
8. Abdulrazzaq, M.M., Noah, S.A., Fadhil, M.A.: X-Ray medical image classification based on multi classifiers. In: IEEE International Conference on Advanced Computer Science Applications and Technologies, pp. 218–223 (2015)
9. Zheng, K.: Content based image retrieval for medical image. In: Proceedings of the IEEE International Conference on Computational Intelligence and Security, pp. 219–222 (2015)
10. Lijuan, S., Fengqi, H.: Research on color and texture feature based image retrieval. In: IEEE International Conference on Intelligent, Transportation, Big Data and Smart City, pp. 626–628 (2015)

11. Kumar, T.G.S., Nagarajan, V.: Local smoothness pattern for content based image retrieval. In: IEEE International Conference on Communications and Signal Processing, pp. 1190–1193 (2015)
12. Jyothi, B., Madhavee Latha, Y., Mohan, P.G.K.: An effective multiple visual features of content based medical image retrieval. In: Proceedings of the 9th IEEE International Conference on Intelligent Systems and Control, pp. 1–5 (2015)
13. Rocha, R., Saito, P.T.M., Bugatti, P.H.: Exploiting revolutionary approaches for content based image retrieval. In: International Symposium on Computer Based Medical System, pp. 370–372 (2015)
14. Gupta, N.M.R.: Comparative analysis of medical images fusion using different fusion methods for Daubechies complex wavelet transform. *Int. J. Adv. Res. Comput. Sci. Softw. Eng.* **3**(6) (2013)
15. Gupta, A., Gangadharappa, M.: Image retrieval based on color, shape and texture. In: 2nd IEEE International Conference on Computing for Sustainable Global Development, pp. 2097–2103 (2015)
16. Bhagyalakshmi, A., Vijayachamundeeswari, V.: A survey on image retrieval using various operators In: IEEE International Conference on Computer Communication and Systems, pp. 18–23 (2014)
17. Wang, Y., Li, Q., Lan, T., Chen, J.: A comparison of image based image retrieval system. In: 17th IEEE International Conference on Computational Science and Engineering, pp. 669–673 (2014)
18. Jenni, K., Mandala, S.: Pre-processing image database for efficient content based image retrieval. In: IEEE International Conference on Advances in Computing, Communications and Informatics, pp. 968–972 (2014)
19. Shriwas, M.K., Raut, V.R.: Content based image retrieval: a past, present and new feature descriptor. In: IEEE International Conference on Circuit, Power and Computing Technologies, pp. 1–7 (2015)
20. Mendoza, O., Melin, P., Licea, G.: A new method for edge detection in image processing using interval type-2 fuzzy logic. In: IEEE International Conference on Granular Computing, pp. 151–155 (2007)
21. Anandakrishnan, N., Santhosh Baboo, S.: An evaluation of popular edge detection techniques in digital image processing. In: IEEE International Conference on Intelligent Computing Applications, pp. 213–217 (2014)
22. Selvakar, P., Hariganesh, S.: The performance analysis of edge detection algorithms for image processing. In: IEEE International Conference on Computing Technologies and Intelligent Data Engineering, pp. 1–5 (2016)
23. Vijaya, A., Sunderesan, M.: Significant image enhancement techniques for removal of noise in LiDar images. In: 3rd International IEEE Conference on Computing for Sustainable Global Development, pp. 3904–3908 (2016)